

# Stereo Vision-Based Self-Localization System for RoboCup

Jen-Shiun Chiang  
Department of Electrical  
Engineering  
Tamkang University  
New Taipei city, Taiwan  
chiang@ee.tku.edu.tw

Chih-Hsien Hsia  
Department of Electrical  
Engineering, National  
Taiwan University of  
Science and Technology  
Taipei city, Taiwan  
chhsia@ee.tku.edu.tw

Hung-Wei Hsu  
Department of Electrical  
Engineering  
Tamkang University  
New Taipei city, Taiwan  
hung.weiwei.hsu@gmail.com

Chun-I Li  
Department of Electrical  
Engineering  
Tamkang University  
New Taipei city, Taiwan  
698450417@s98.tku.edu.tw

**Abstract**—This work proposes a new Stereo Vision-Based Self-Localization System (SVBSLS) for the RoboCup soccer humanoid league rules for the 2010 competition. The humanoid robot integrates the information from the pan/tilt motors and stereo vision to accomplish the self-localization and measure the distance of the robot and the soccer ball. The proposed approach uses the trigonometric function to find the coarse distances from the robot to the landmark and the robot to the soccer ball, and then it further adopts the artificial neural network technique to increase the precision of the distance. The statistics approach is also used to calculate the relationship between the humanoid robot and the position of the landmark for self-localization. The experimental results indicate that the localization system of SVBSLS in this research work has 100% average accuracy ratio for localization. The average error of distance from the humanoid soccer robot to the soccer ball is only 0.64 cm.

**Keywords**- Back propagation neural network; humanoid robot; Robo Cup 2010; self-localization, stereo vision

## I. INTRODUCTION

The research of robots is one of the most important issues in recent years. In the numerous robot researches, the development of autonomous robots is attracted mostly. Accompanying the advancement of robotics and artificial intelligence, the autonomous robots cannot only handle simple and monotonous problems, but also have independent thoughts to deal with the complex states in the unpredictable and dynamic environments. All these functions rely on a powerful vision system, and therefore the vision system is one of the most critical techniques for the autonomous robot system. In the RoboCup soccer humanoid league competition, the vision system is used to collect various environment information as the terminal data to finish the functions of object recognition, coordinate building, robot localization, robot tactic, barrier avoiding, etc. A good self-localization system for a humanoid soccer robot cannot only make the robot acquire the information quickly and accurately in the whole field, but also make an appropriate decision correspondingly. For easy manipulation we can preset all the locations in the field as a Cartesian coordinate system, and the robot will self-localize itself by the coordinate system. In recent years, the competition fields of RoboCup [1] and FIRA

Cup [2] become more and more conformed to human environments. Fig. 1 shows the RoboCup soccer fields for humanoid kid-size of 2009 and 2010, respectively. The sizes of the landmark pole and landmark goal in the field become smaller [3-4]. In other words, the reference checkmarks for self-localization become less and less, and how to use less landmarks and increase the degree of accuracy become important issues [5-6].

Zhong et al. [7] proposed three types of techniques for robot localization. The first approach is based on the stereo vision. This approach can obtain a lot of information such that the distance measurement between the camera and the target is accurate enough [8] to increase the accuracy of localization. The second one is based on the omni-directional vision. Although this method obtains better features, the omni-directional device causes geometry distortions to the perceived scene [9]. The third one uses the monocular vision technique. However, it must have robust features within a specific region [10]. SLAM [11] is an algorithm for localization and mapping simulation and is appreciated by many researchers. Although this algorithm has better efficiency, it needs complex image processing procedures and is difficult to be applied to the embedded system for real time humanoid soccer robot applications. For the implementation of the humanoid soccer robot, real time is the main issue, and we need a less complicated but high efficient localization method. Therefore for the humanoid soccer robot competition purpose, we propose a visual self-localization approach, stereo vision-based self-localization system (SVBSLS), which uses two CCD cameras and a set of pan/tilt motors on the robot head to find the various features and analyze the environmental information of the RoboCup 2010 soccer field [4].

The rest of this paper is organized as follows. Section II presents the related background such as the general color based object recognition methods, intrinsic parameters of the CCD, and distance measurement. Section III describes the proposed approach, SVBSLS. The experimental results of SVBSLS applied to the humanoid soccer robot are described in Section IV. Section V compares and analyzes the self-localization for humanoid robot by SVBSLS and other approaches. Finally, Section VI gives a brief conclusion.

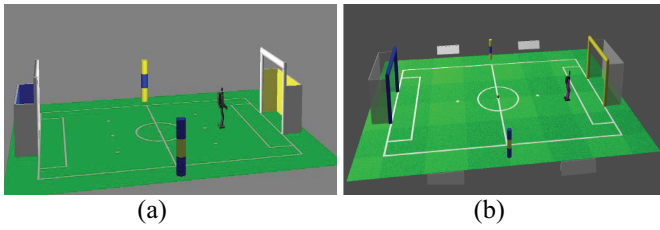


Figure 1. The configuration of RoboCup soccer fields for humanoid kid-size: (a) for 2009, (b) for 2010.

## II. BACKGROUND

### A. Intrinsic Parameters of the CCD Camera

The vision-based distance measurement needs the intrinsic parameters, such as focal distance and horizontal viewpoints, of the CCD camera. Generally the camera makers rarely provide such parameters. Even if they provide such parameters, the mechanical mechanism, processing circuits, and lens distortion may cause deviations of the parameters. Actually we can find the intrinsic parameters of the CCD cameras regardless of the CCD brandes.

The relationship of the distance between the CCD camera and the object and some parameters are shown in Fig. 2. In Fig. 2,  $OP$  is the optical origin;  $2\theta_H$  is the horizontal viewpoints, and  $D_{OP}$  is the distance between  $OP$  and the edge of the CCD lens.

In order to find the distance between the CCD center and the object,  $\theta_H$  and  $D_{OP}$  must be found first. We can capture the width of an object,  $D_{H1}(max)$ , with a pre-defined position,  $D_A$ , and the width of the same object,  $D_{H2}(max)$ , with a pre-defined position,  $D_B$ . The two captured frames can be combined to form Fig. 3. By the trigonometric functions we can derive  $\theta_H$  in (1):

$$\theta_H = \cot^{-1} \left( 2 \times \frac{D_{K2} - D_{K1}}{D_{H2}(max) - D_{H1}(max)} \right) \quad (1)$$

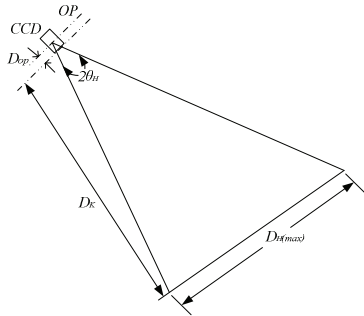


Figure 2. The internal parameters diagram of a CCD camera. By the theorem of similar triangles,  $D_{OP}$  can be found as shown in (2) and (3).

$$\frac{D_{OP} + D_{K1}}{D_{OP} + D_{K2}} = \frac{D_{H1}(max)}{D_{H2}(max)} \quad (2)$$

$$D_{op} = \frac{D_{K2}D_{H1}(max) - D_{K1}D_{H2}(max)}{D_{H2}(max) - D_{H1}(max)} \quad (3)$$

The above approach can be applied to find the intrinsic parameters for any kind of CCD cameras. Once  $D_{OP}$  is found, the distance between the camera and the object can be

measured by IBDMS (image-based distance measuring system) [12-13].

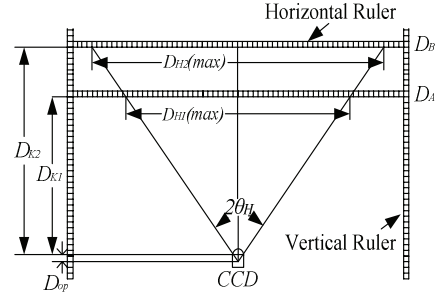


Figure 3. The intrinsic parameters measuring system[12-13].

### B. Image-Based Distance Measuring System (IBDMS) [12-13]

The IBDMS (image-based distance measuring system) uses two fixed lasers to project the laser beams to the object to measure the distance between the CCD camera and the object. Fig. 4 is the diagram of the location relationship of the CCD camera and the object. The unit of  $D_{SH}$  is cm that is the actual length of the distance between the two lasers.  $F_H$  is the pixel numbers that the laser beams project to the object in a picture frame. If the maximum horizontal pixels that a CCD camera can catch in a picture frame is  $F_H(max)$ , the maximum width (in cm as unit) that a CCD camera can reach can be calculated as (4):

$$D_H(max) = \frac{F_H(max)}{F_H} \times D_{SH} \quad (4)$$

According to Fig. 4, the distance  $D_K$  (with unit of cm) between the CCD camera and object can be calculated with the intrinsic CCD parameters as mentioned in the previous subsection as (5):

$$D_K = \frac{1}{2} \times D_H(max) \times D_{SH} \times \cot\left(\frac{\theta_H}{2}\right) - D_{op} \quad (5)$$

In the RoboCup 2010 rule, the landmark pole is a cylinder with diameter equal to 10cm. when the IBDMS is applied to measure the distance between the CCD camera and the landmark pole, the two lasers of the original IBDMS can be removed, and we call this approach without lasers as modified IBDMS.

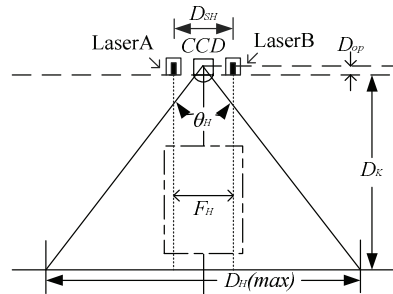


Figure 4. The location relationship of the CCD camera and the object.

### III. THE PROPOSED METHOD

This research work uses the parallax of a stereo (binocular) vision system to establish the stereo vision-based self-localization system (SVBSLS) for a humanoid soccer robot used in the Robo-Cup 2010 kid-size humanoid robot soccer competition. Basically there are two main issues in this research: 1) how to utilize the landmarks, such as the landmark poles and landmark goals, of the competition field to find the coordinate of the humanoid robot in a 2-D coordinate system, 2) how to measure the accurate distance of the humanoid robot and the soccer ball. Here we have to overcome the difficulties caused by the CCD camera intrinsic parameters such as focal distance and visual angle. The humanoid soccer robot can be adjusted by the tactics dynamically, such as localizing before competition, measuring the distance of the robot and the soccer ball during competition, or localizing during competition.

For the localization algorithm, it needs several procedures: establishment of the coordinate system, object searching, object identification, the distance measurement between the robot and object, refinement of the measured distance, and the adjustment of the location of the robot and the landmarks. In the distance measurement, we use the modified IBDMS approach and the parallax of the stereo vision system. For precision and convenience considerations, the soccer field is treated in a 2-D coordinate system. In the object detection, the two cameras of the stereo vision system catch images in RGB 24-bit colorful formats, respectively. The RGB images are then converted to the HSV colorful formats, and here we only utilize  $H$  and  $S$  data and further convert them to the binarization format with proper threshold values. The binarization data are processed to reduce noises to increase the correctness and integrity for object recognition. According to the processed binarization data we can distinguish the object as landmark pole, landmark goal, or soccer ball. If the object is a landmark pole or landmark goal, it will try to localize the robot itself and output the coordinate values to the system. If the object is a soccer ball (we call this as a distance mode), it will try to measure the distance between the robot and soccer ball and output the distance value to the system.

#### A. Establishment of the Coordinate System

If the coordinate of a geometric map is available, it will be convenient to retain a lot of information in the whole field. For easy manipulation of the self-localization of a robot, the coordinate system of the field must be established in advance. In this research work, before processing the localization we must establish two appropriate coordinate systems. One is called "absolute coordinate system" on the field, and the other is called "relative coordinate system" in the picture frame. It needs four steps to establish the absolute coordinate system: 1) to estimate the sizes of the soccer field and the robot; 2) to find the interested position in the soccer field; 3) to divide the field into several blocks with the same size and assign the interested position block; 4) according to the proportion of the robot in the field to adjust the value in each block. Through these coordinate systems, the location of the robot, landmark pole, and landmark goal can be located explicitly.

#### B. Object Searching

Since the objects (landmark poles and landmark goals) are the fixed features in the 2010 RoboCup soccer field, we treat the objects as the reference for localization. In the initialization of the orientation, the robot keeps searching one of the objects until finding it. After finding the object, the two cameras of the system will take the interested feature by converting the image from RGB to HSV space, respectively, as shown in Fig. 5. In order to remove the influence of brightness of light, it takes the  $H$ - and  $S$ - spaces only. Finally, each camera will mark five feature points, upper left ( $X_1, Y_1$ ), upper right ( $X_2, Y_2$ ), lower left ( $X_3, Y_3$ ), lower right ( $X_4, Y_4$ ), and center ( $X_C, Y_C$ ), for the object in the picture frame, as shown in Fig. 6. According to the five feature points in each picture frame, we can calculate the horizontal lengths (in pixels)  $FH_{Lx}$ ,  $FH_{Rx}$  and vertical lengths  $FH_{UPx}$ ,  $FH_{DOWNx}$  (where  $x$  is either 1 or 2; 1 represents the left camera, and 2 represents the right camera) for each of the two cameras. The parallax (in pixels) of the two cameras can be calculated as follows:

$$\Delta N = |FH_{L1} - FH_{L2}| = |FH_{R1} - FH_{R2}| \quad (6)$$

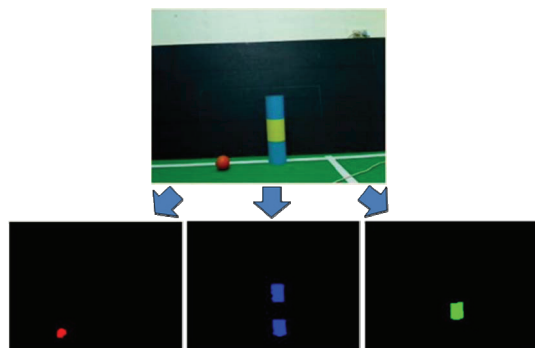


Figure 5. Color model transformation.

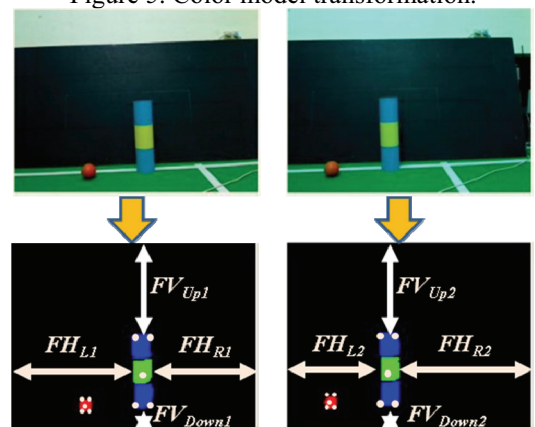


Figure 6. The upper left, upper right, lower left, lower right, and center of the object in the two cameras.

#### C. Object Recognition Method

According to the color segmentation method, it can fast and easily extract the orange soccer ball in the field, but it is not enough to recognize the landmark goals and landmark poles. The colors of the landmark goals and landmark poles are yellow and blue, and by color segmentation the extraction of the landmark goals and landmark poles may not be correct as shown in Fig. 7. Therefore we have to use more features and

information to extract them. Since the competition field is not complicated, a simple recognition method can be used to reduce the computation complexity. The landmark pole is a cylinder with three colors. Let us look at one of the landmark pole with the upper and bottom layers in blue, and the center layer in yellow; this one is defined as the BYB-landmark pole, and the diagram is shown in Fig.8. The color combinations of the other one are in contrast of the previous one, and the landmark pole is defined as the YBY-landmark pole. The labels of the BYB-landmark pole can be calculated by (7). The YBY landmark pole is in the same manner as the BYB-landmark pole.

$$O_{BYB}(x, y) = L_B^u(x, y) + L_B^v(x, y) + L_Y^w(x, y) \quad (7)$$

$$\text{if } |L_B^u(x_c) - L_B^v(x_c)| < \beta \cap L_B^u(y_{\max}) < L_Y^w(y_c) < L_B^v(y_{\min})$$

where  $L_B^u$  is the pixel of the  $u$ -th blue component in a picture frame,  $y_{\min}$  and  $y_{\max}$  the minimum value and the maximum value for the object  $u$  at  $y$  direction in the picture frame respectively,  $x_c$  and  $y_c$  the center point of the object at the horizontal and vertical direction respectively. The vertical bias value  $\beta$  is set as 45 empirically. The landmark pole is composed of two same color objects in the vertical line, and the center is in different color. If it can find an object with this feature, the system treats this object as the landmark pole and outputs the frame coordinate data. Equation (8) is used to define the label of the soccer ball.

$$O(x, y) = L_O^u(x, y), \text{ if } \alpha_1 \leq \frac{L_O^u(x_{\max}) - L_O^u(x_{\min})}{L_O^u(y_{\max}) - L_O^u(y_{\min})} \leq \alpha_2 \cap A_u \text{ is the maximum} \quad (8)$$

where  $L_O^u$  is the pixel of the  $u$ -th orange component in a picture frame. Since the soccer ball is very small in the picture frame, in order to avoid the noise the soccer ball is treated as the maximum orange object and with a shape ratio of height to width approximately equal to 1. Empirically  $\alpha_1$  and  $\alpha_2$  are set to 0.8 and 1.2, respectively. The landmark goal recognition is defined in (9).

$$G_B(x, y) = L_B^u(x, y),$$

$$\text{if } L_B^u(x, y) \notin O_{BYB}(x, y) \cap L_B^u(x, y) \notin O_{YBY}(x, y) \cap A_B^u > \gamma_B \quad (9)$$

where  $L_B^u$  is the pixel of the  $u$ -th blue component in a picture frame. Since the blue landmark goal is composed of the blue object and it is not a part of the YBY-landmark pole or BYB-landmark pole. The size of the landmark goal in the field is larger than other objects, and empirically the parameter  $\gamma$  is set as 50. The yellow landmark goal is in the same manner as the blue landmark goal.

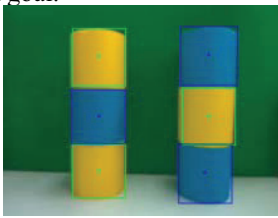


Figure 7. False segmentation of the landmark pole.

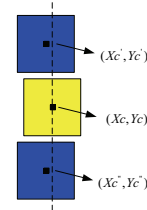


Figure 8. The diagram of the landmark pole.

To get robust  $FH_L$ ,  $FH_R$ ,  $FH_{UP}$ , and  $FH_{DOWN}$ , the object shape must be completely displayed in the picture frame, as shown in Fig. 9(b). Figs. 9(a) and 9(c) show the incomplete objects with partial object displayed in the picture frame. If it finds an incomplete object in the picture frame or the object could be occluded by other robots, the system will command the robot to activate some proper movements to find a complete object. In order to insure the completeness of the object, the pixel values between the edge of the object and the edge of the frame should be greater than some appropriate values.

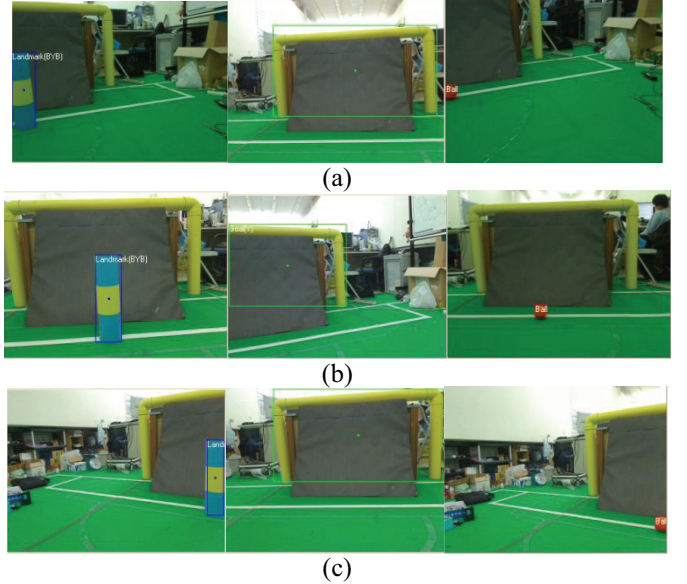


Figure 9. Object searching: (a) incomplete object, (b) complete object, (c) incomplete object.

#### D. Distance Measurement between the Robot and Object

The distance measurement between the robot and the object is based on the parallax of the stereo vision. The modified IBDMS as mentioned in the previous section is applied to measure the distance between the CCD camera and object (the landmark pole, landmark goal, or soccer ball) for the RoboCup 2010 rule. Fig. 10 shows the relationship of the camera and the object. In Fig. 10,  $\Delta h$  is the length of the distance between the two cameras and  $D_H$  is the parallax in unit of cm.  $D_H$  can be converted by the parallax  $\Delta N$  (in pixels) and  $\Delta h$  as follows:

$$D_H = \frac{\Delta h \times F_H(max)}{\Delta N} \quad (10)$$

where  $F_H(max)$  is the maximum horizontal pixels that a camera can reach in a picture frame.  $FH_{L1}$ ,  $FH_{R1}$ , and  $FH_{L2}$ ,  $FH_{R2}$  are the lengths in pixels for horizontal lengths of the landmark pole in the image frame. By the modified IBDMS

approach, the distance  $D_K$  (photo-distance) between the CCD camera and the landmark can be found as follows:

$$D_K = \frac{1}{2} \times D_H \times \cot \theta_H - D_{OP} \quad (11)$$

Due to the non-ideality of the CCD lens and the light illumination the measurement of  $D_K$  may not be accurate enough. It can be fine-tuned by the artificial neural network technique. The neural network technique is described in the following subsection.

#### E. Stereo Vision-based Self-localization System (SVBSLS)

Based on the above concepts, the self-localization system, stereo vision-based self-localization system (SVBSLS), is proposed for the humanoid soccer robot for RoboCup 2010 competition. The proposed SVBSLS consists of six steps, and the operation flow of this self-localization mechanism is shown in Fig. 11. The six steps are:

- Step 1: Establish the coordinate system.
- Step 2: Search objects.
- Step 3: Recognize objects.
- Step 4: Measure the distance between the robot and objects.
- Step 5: Fine-tune the measured distance.
- Step 6: Find the coordinate of the robot in the competition field.

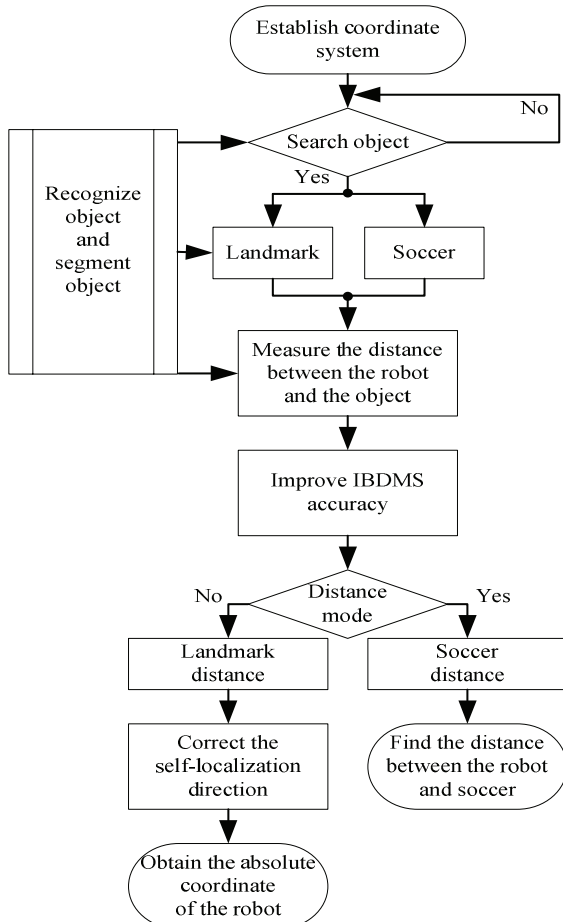


Figure 11. The SVBSLS flowchart for the humanoid robot.

## IV. THE EXPERIMENT RESULTS

### A. The Experimental Environment and the Robot Vision Module

The experiments are based on the feature of the competition field for 2010 RoboCup soccer humanoid league. The field contains two landmark goals and two landmark poles, and it has unique color combinations for the interesting features as shown in Fig. 12. Because the width of the robot shoulder is 26cm, we set the unit length of the coordinate to be 30cm in length and the competition field can be divided into  $29 \times 17$  blocks as shown in Fig. 13.

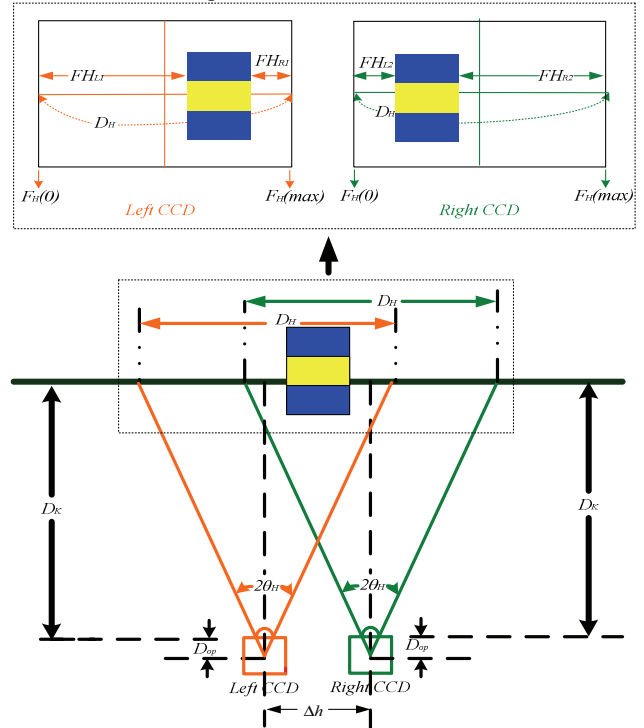


Figure 10. Three-dimension distance measurement.

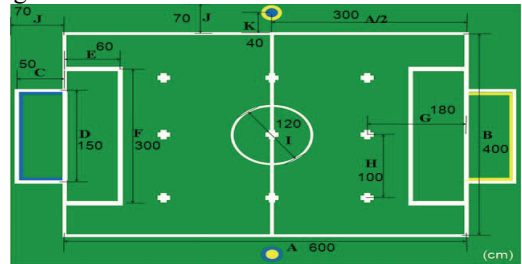


Figure 12. Configuration of the RoboCup soccer field for humanoid kid-size in 2010.

The experimental robot vision module is consisted of two CCD cameras with distance of 10cm and a set of pan/tilt motors. The CCD camera is the Logitech QuickCam® Professor [14] for Notebooks, and the motor is ROBOTIS Dynamixel AX-12 [15]. The input of the robot vision module is RGB 24-bit and the resolution is  $960 \times 720$  pixels, and the frame rate is 4 fps (frame per second). For simulation, the computer CPU is Intel Core 2 Duo CPU 2.1GHz, and the development tool is Borland C++ Builder 6.0. The output is the

absolute coordinate of the humanoid robot in the competition field.

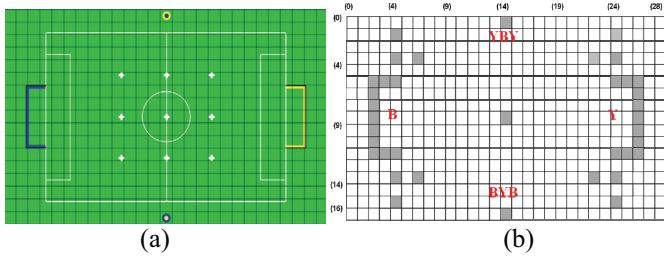


Figure 13. The RoboCup soccer field: (a) the original field with 29×17 blocks, (b) the coordinate of the soccer field (2010).

### B. The Parallax $\Delta N$ of Stereo Vision Analyses

We measured the parallax  $\Delta N$  in a given distance with different pan/tilt motor angles, and the results are shown in Table 1. According to Table 1, as the same distance the parallax  $\Delta N$  is the same with different pan/tilt motor angles. Therefore, our SVBSLS does not need to calibrate the non-linear distortion caused by the visual angle of the lens, and it can measure the distance of the object as soon as the camera sees the complete object in the picture frame.

Table 1. The parallax  $\Delta N$  of the landmark pole in a given distance with different pan/tilt motor angles. (a) The parallax  $\Delta N$  of the landmark pole in a given distance with different pan motor angles. (b) The parallax  $\Delta N$  of the landmark pole in a given distance with different tilt motor angles.

$D_k^{angle}$	-20	-15	-10	-5	0	5	10	15	20
50	148	148	148	148	148	148	148	148	148
100	76	76	76	76	76	76	76	76	76
150	52	52	52	52	52	52	52	52	52
210	36	36	36	36	36	36	36	36	36
270	28	28	28	28	28	28	28	28	28

(a)

$D_k^{angle}$	-20	-15	-10	-5	0	5	10	15	20
60	128	128	128	128	128	128	128	128	128
90	84	84	84	84	84	84	84	84	84
120	64	64	64	64	64	64	64	64	64
150	52	52	52	52	52	52	52	52	52
180	40	40	40	40	40	40	40	40	40
210	36	36	36	36	36	36	36	36	36
240	32	32	32	32	32	32	32	32	32
270	28	28	28	28	28	28	28	28	28
300	24	24	24	24	24	24	24	24	24

(b)

### C. Precision Simulation of the Distance Measurement

For the BPN network approach, we need data for the two neurons in the input layer ( $\Delta N$  and the rough distance  $D_K$ ) to

measure the distance to the landmark and the input layer ( $\Delta N$  and rough distance  $D_K$ ) to measure the distance to the soccer ball. The total training samples are 247. The hidden layer is one. Because the absolute coordinate system of the soccer field is fixed, we can train the on-line data beforehand. The simulation result indicates that the most suitable number of neurons is six. The learning rate is 0.1, and the output layer is one. After finishing the on-line training, the relationships between the information of the frame and the distance can be found, and then it can operate the off-line process for the invariable parameters (relationships) to improve the precision of the distance. The precision can reach 0.028cm for the landmark distance measurement and 0.005cm for the soccer ball distance measurement, and the simulation results are shown in Fig. 14.

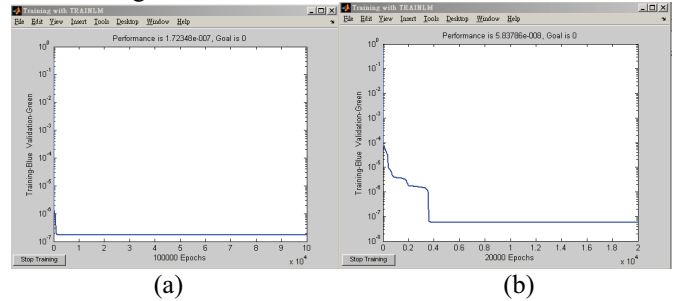
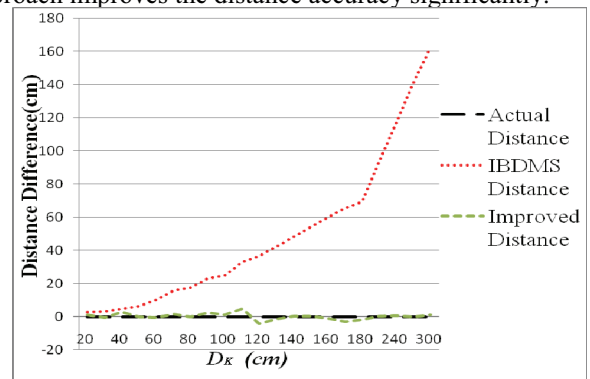


Figure 14. The errors between the simulated and real distances are: (a) 0.028cm in the landmark distance measurement and (b) 0.005cm in the soccer ball distance measurement.

## I. COMPARISONS AND ANALYSES

### A. The Analyses for the Actual Measuring Distance

This work uses modified IBDMS and NNIBDMS techniques to measure the distance between the robot and landmark and the distance between the robot and soccer ball from 10cm to 300cm. Fig. 15 shows the errors between the measuring distance and actual distance, and the results are listed in Table 2. In the distances from 10cm to 300cm, the average and maximum errors for the modified IBDMS are 48.96cm, 51.03cm, and 162.16cm, 170.52cm, respectively. On the other hand, those of the NNIBDMS are 1.38cm, 0.64cm, and 2.49cm, 4.55cm, respectively. The proposed NNIBDMS approach improves the distance accuracy significantly.



(a)

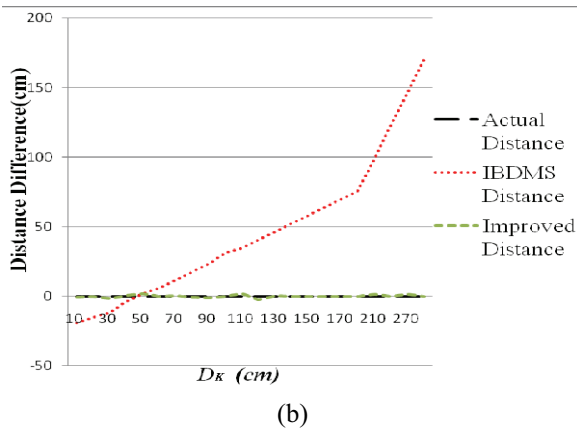


Figure 15. The distance differences of the actual distance and the modified IBDMS and NNIBDMS approaches, (a) Landmark distance, (b) Soccer ball distance.

Table 2. Comparisons of the maximum and average errors for different methods.

Landmark distance		
Methods	Average error	Maximum error
Modified IBDMS	48.96 cm	162.16 cm
NNIBDMS	1.38 cm	4.55 cm
Soccer ball distance		
Methods	Average error	Maximum error
Modified IBDMS	51.03 cm	170.52 cm
NNIBDMS	0.64 cm	2.49 cm

### B. The Results of the Self-localization in the Competition Field

The distances measured between the robot and landmarks as mentioned in the previous subsection are applied to the SVBSLS to localize the robot itself. The localization results of using the distances measured by the modified IBDMS and NNIBDMS are compared. The experiments include the localization by using the distance from the robot to the landmark pole and the distance from the robot to the landmark goal. There are 247 coordinate positions in Fig. 16. The yellow and blue star signs stand for the correct localization by using the NNIBDMS approach for distance measurement. The purple star signs stand for the correct localization by using the modified IBDMS or NNIBDMS approaches for distance measurement. The red star signs stand for the correct localization with both landmark pole and landmark goal by using the NNIBDMS approach for distance measurement. Table 3 shows the comparisons for the robot localization by using SVBSLS with modified IBDMS and NNIBDMS approaches for distance measurement. The correct rate for the SVBSLS approach with the NNIBDMS approach is 100%; on the other hand that of the localization by the modified IBDMS is only 13.77%. The main reason of the lower correct rate is due to the worse accurate measuring distance results.

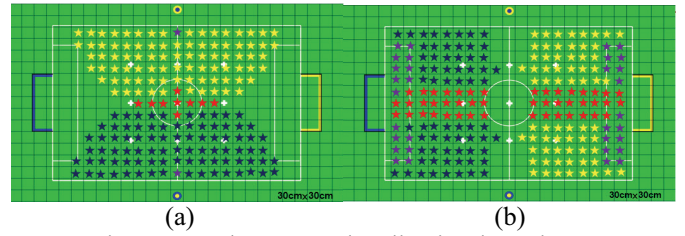


Figure 16. The correct localization by using SVBSLS with modified IBDMS and NNIBDMS approaches, (a) Landmark pole, (b) Landmark goal.

Table 3. Comparisons of the correct rates for SVBSLS with different distance measurement methods.

Total experimental points = 247(blocks)			
Situation	Correct	Incorrect	Accuracy rate
IBDMS	34	213	13.77%
SVBSLS	247	0	100%

### C. The Comparisons of Monocular Vision and Binocular Vision

In this subsection we compare the localization results of SVBSLS approach with those of the monocular vision approach, AVBSLS [16], under the same experimental environment. The errors of the distance measurement by the NNIBDMS approach with monocular vision (AVBSLS) and binocular vision (SVBSLS) are shown in Fig. 17. The results are summarized in Table 4. The average and maximum errors of the distance measurement by AVBSLS are 2.68cm and 12.86cm, respectively. On the other hand, those by SVBSLS are 1.38cm and 4.55cm, respectively. The proposed SVBSLS approach increases the distance measurement accuracy significantly.

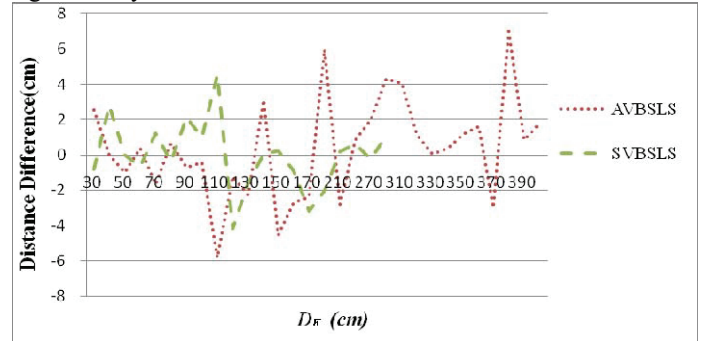


Figure 17. The distance errors by using AVBSLS and SVBSLS.

The correctness of the localization by using AVBSLS and SVBSLS is shown in Fig. 18 with 247 coordinate positions. The red star signs stand for the correct localization results. Table 5 shows the correct rates of the localization by using AVBSLS and SVBSLS approaches. The correct localization rate of the AVBSLS is 93.5%, but it must have robust features within a specific region. On the other hand, the SVBSLS approach can have a 100% correct rate without any restriction.

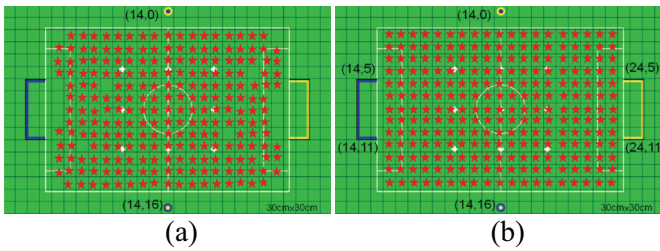


Figure 18. The localization results of AVBSLS and SVBSLS, (a) AVBSLS, (b) SVBSLS.

Table 4. The average and maximum errors of the distance measurement by AVBSLS and SVBSLS.

Landmark		
Methods	Average error	Maximum error
AVBSLS	2.68 cm	12.86 cm
SVBSLS	1.38 cm	4.55 cm

Table 5. The comparisons of the correct localization rate with AVBSLS and SVBSLS.

Total experimental points = 247(blocks)			
Situation	Correct	Incorrect	Accuracy rate
AVBSLS	231	16	95.5%
SVBSLS	247	0	100%

## CONCLUSIONS

Self-localization is one of the most important issues for the humanoid soccer robot. This research work proposes a very efficient vision approach, stereo vision-based self-localization system (SVBSLS), to localize the soccer robot itself during the soccer competition for the 2010 RoboCup rule. In order to emulate the human being, the mechanism of the SVBSLS consists of only two CCD cameras and a set of pan/tilt motors on the head of the humanoid soccer robot. We use the landmarks of the soccer field as the reference points to correctly self-localize the humanoid robot. In the SVBSLS approach, we have to measure the distance between the robot and the landmark. The modified IBDMS approach is used to measure the intrinsic parameters of the CCD camera and further to calculate the distance between the robot itself and the landmark or soccer ball. The BPN technique is used to refine the calculated distance to a more accurate one (NNIBDMS). By the SVBSLS approach with the NNIBDMS technique, the accuracy rate of the self-localization of the humanoid soccer robot can reach 100%, the average error of distance from the humanoid soccer robot to the soccer ball is only 0.64cm. Since the resolution of the CCD camera is 960×720 pixels, the frame rate is only 4 fps. Although it is enough for the robot soccer competition, the computation efficiency can be improved by using the technique of hardware acceleration. The bottleneck (such as the color transform) can be overcome by hardware approach, and the

image processing can be improved such that the robot can operate more smoothly.

## ACKNOWLEDGEMENT

This work was supported by the National Science Council of Taiwan, R.O.C. under grant number: NSC 98-2218-E-032-003.

## REFERENCES

- [1] H. Kitano, M. Asada, Y. Kuniyoshi, I. Noda, and E. Osawa. "Robocup: The robot world cup initiative," IJCAI-95 Workshop on Entertainment and AI/ALife, pp. 19-24, 1995.
- [2] FIRA RoboWorld Congress, 2010, Available: <http://www.fira.net>.
- [3] RoboCup Soccer Humanoid League Rules and Setup for the 2009 competition, 2009 Available: <http://www.robocup2009.org/>
- [4] RoboCup Soccer Humanoid League Rules and Setup for the 2010 competition, 2010 Available: <http://www.robocup2010.org/>
- [5] I. Shimshoni, "On mobile robot localization from landmark bearings," IEEE Transactions on Robotics and Automation, vol. 18, no. 6, pp. 971-976, December 2002.
- [6] M. Betke and L. Gurvits, "Mobile robot localization using landmarks," IEEE Transactions on Robotics and Automation, vol. 13, no. 2, pp. 251-263, April 1997.
- [7] Z.-G. Zhong, J.-Q. Yi, D.-B. Zhao, Y.-P. Hong, and X.-Z. Li, "Motion vision for mobile robot localization," IEEE International Conference on Control, Automation, Robotics and Vision, vol. 1, pp. 261-266, December 2004.
- [8] D.-J. Kriegman, E. Triendl, and T.-O. Binford, "Stereo vision and navigation in buildings for mobile robots," IEEE Transactions on Robotics and Automation, vol. 5, no. 6, pp. 792-802, Dec. 1989.
- [9] S.-K. Choi, J. Yuh, and G.-Y. Takashige, "Development of the omnidirectional intelligent navigator," IEEE Robotics & Automation Magazine, vol. 2, no. 1, pp. 44-53, Mar. 1995.
- [10] P.-R. Liu, M.-Q. Meng, and P.-X. Liu, "Moving object segmentation and detection for monocular robot based on active contour model," Electronics Letters, vol. 41, no. 24, Nov. 2005.
- [11] J. Kim, K.-J. Yoon, J.-S. Kim, and I. Kweon, "Visual SLAM by single-camera catadioptric stereo," SICE-ICASE International Joint Conference, pp. 2005-2009, Oct. 2006.
- [12] S. Karin and P. Ioannis, "A novel method for automatic face segmentation, facial feature extraction and tracking," Signal Processing: Image Communication, vol. 12, no. 3, pp. 263-281, Jun. 1998.
- [13] N. Herodotou, K. N. Plataniotis, and A. N. Venetsanopoulos, "Automatic location and tracking of the facial region in color video sequences," Signal Processing: Image Communication, vol. 14, pp. 359-388, 1999.
- [14] C.-C. Chen, M.-C. Lu, C.-T. Chuang, and C.-P. Tsai, "Vision-based distance and area measurement system," IEEE Sensors Journal, vol. 6, no. 2, pp. 495-503, Apr. 2006.
- [15] C.-C. Hsu, M.-C. Lu, W.-Y. Wang, and Y.-Y. Lu, "Distance measurement based on pixel variation of CCD images," ISA Transactions, vol. 48, issue 4, pp. 389-395, Oct. 2009.
- [16] Logitech, 2007, Logitech QuickCam® Pro for Notebooks, Available : <http://www.logitech.com/>
- [17] Robotis, 2006, ROBOTIS Dynamixel AX-12, Available : [http://www.robotis.com/zbxe/software\\_en](http://www.robotis.com/zbxe/software_en).
- [18] S.-H. Chang, W.-H. Chang, C.-H. Hsia, F. Ye, and J.-S. Chiang, "Efficient neural network approach of self-localization for humanoid robot," Joint Conference on Pervasive Computing, pp. 149-154, Dec. 2009.